Lg AMPLITUDE RATIOS FROM PEACEFUL NUCLEAR EXPLOSIONS AND CRUSTAL STRUCTURE IN NORTHERN EURASIA

Hongyan Li[1], Igor B. Morozov[1, 2], and Scott B. Smithson[1]

University of Wyoming[1], University of Saskatchewan[2]

Sponsored by Air Force Research Laboratory

Contract No. DTRA01-01-C-0057

ABSTRACT

The *Lg* phase is widely used in Comprehensive Nuclear-Test-Ban Treaty (CTBT) monitoring since it is usually the strongest at regional distances. However, studies of its amplitude variability have revealed that the *Lg* phase can be attenuated or even blocked in some continental areas. Consequently, it is important to study the key factors that affect the *Lg* phase propagation across tectonic and geological boundaries. For Northern Eurasia, an unparalleled dataset for such analysis is the historic Peaceful Nuclear Explosion Deep Seismic Sounding (PNE DSS) program. Dense (10-20-km spacing), short-period (0.5-20 Hz), three-component PNE recordings of the regional phases have recently become available. In this study, data from 17 PNEs are analyzed for variability of the *Lg*/*Sn* and *Lg*/*Pg* amplitude ratios and their relation to tectonics and crustal structure.

The recorded *Lg* phase energy is mainly concentrated at 0.5-3 Hz, and this band appears to be optimal for calibration. In our PNE datasets, the *Lg* phase is not always the strongest phase, which could be due to the differences in source magnitudes and conditions.

The high density of PNE recordings allowed careful and detailed picking of the phase time windows (*P*, *Pg*, *Sn*, and *Lg*), by contrast with group velocity-based windowing usually employed, and measurement of their amplitudes using several techniques, with measurement uncertainties statistically determined. Further, differential slopes of the phase amplitude ratios were estimated and decomposed into the regional trends and effects of crustal variability.

Lg amplitude ratios along the reversed and crossing PNE profiles show that the *Lg* phase can be strongly attenuated (blocked) by rapid variations in the crustal thickness, such as the Patom Vilyuy Basin with more than 15 km of sediments and over10 km of Moho uplift. Smaller variations of the crustal thickness (e.g., Ural Mountains and Mezenskaya Depression) lead to moderate decay of *Lg* amplitudes. Within sedimentary basins (West Siberian, Timan-Pechora, Low Angara, and Tunguss), the *Lg*/*Sn* ratios decrease with the source-receiver offset. The corresponding decay rates are ~0.001km^{-1} within the Tunguss Basin, ~0.002 km^{-1} within the West Siberian Basin, ~0.002 km^{-1} to ~0.003 km^{-1} within the West Siberian Rift (Ob-Tasovsk Depression) and the Yenisei-Hantanga Basin. By contrast, within cratons with thinner sedimentary covers (East European and Siberian), the ratios increase or stay constant with offset. In addition to correlation with the sediment thickness, *Lg* phase propagation efficiency appears to be affected by the age of the sediments. Younger sediments appear to attenuate the *Lg* phase more strongly than older ones. These correlations are particularly pronounced in the 0.5-3 Hz frequency band, indicating that this band would benefit most from calibration.

OBJECTIVES

The *Lg* phase is usually observed as the strongest of the regional phases and is widely used for nuclear discrimination and studying crustal structure variations. However, the *Lg* phase is totally or partially blocked in some areas. Therefore, studying the characteristics of *Lg*-phase propagation and its main factors are critical for its use in nuclear-test monitoring.

This study analyzes the spectrum characteristics of the *Lg* and *Sn* phases to find the best frequency band for calibration; then computes the *Lg*/*Sn* and *Lg*/*Pgcoda* amplitude ratios with the optimal frequency band to study the variations of the ratios in different geologic areas of Northern Eurasia, in order to constrain the main factors affecting *Lg* propagation.

RESEARCH ACCOMPLISHED

Of all the regional phases, the *Lg* is usually the most prominent and robust in continental regions, and therefore it is widely used to determine regional variations of crustal structure and discriminate nuclear explosions from earthquakes. However, the *Lg* phase can also be highly attenuated or even blocked by abrupt changes in crustal structure; understanding the main factors that affect *Lg* in different crustal structures is crucial to the use of the *Lg* phase in nuclear test monitoring.

Northern Eurasia represents a large and complex geologic area, and therefore is ideal for studying the main factors influencing *Lg* phase propagation in contrasting tectonic areas. However, the means for traditional calibration of this region based on natural sources are limited. Northern Eurasia is largely aseismic, and regional recordings of natural sources are relatively scarce. Also, path calibration of regional seismic phases is strongly dependent on the accuracy of hypo-central locations of calibration events (Saikia et al, 2001), and for earthquakes, especially for small events, this information can be difficult to obtain.

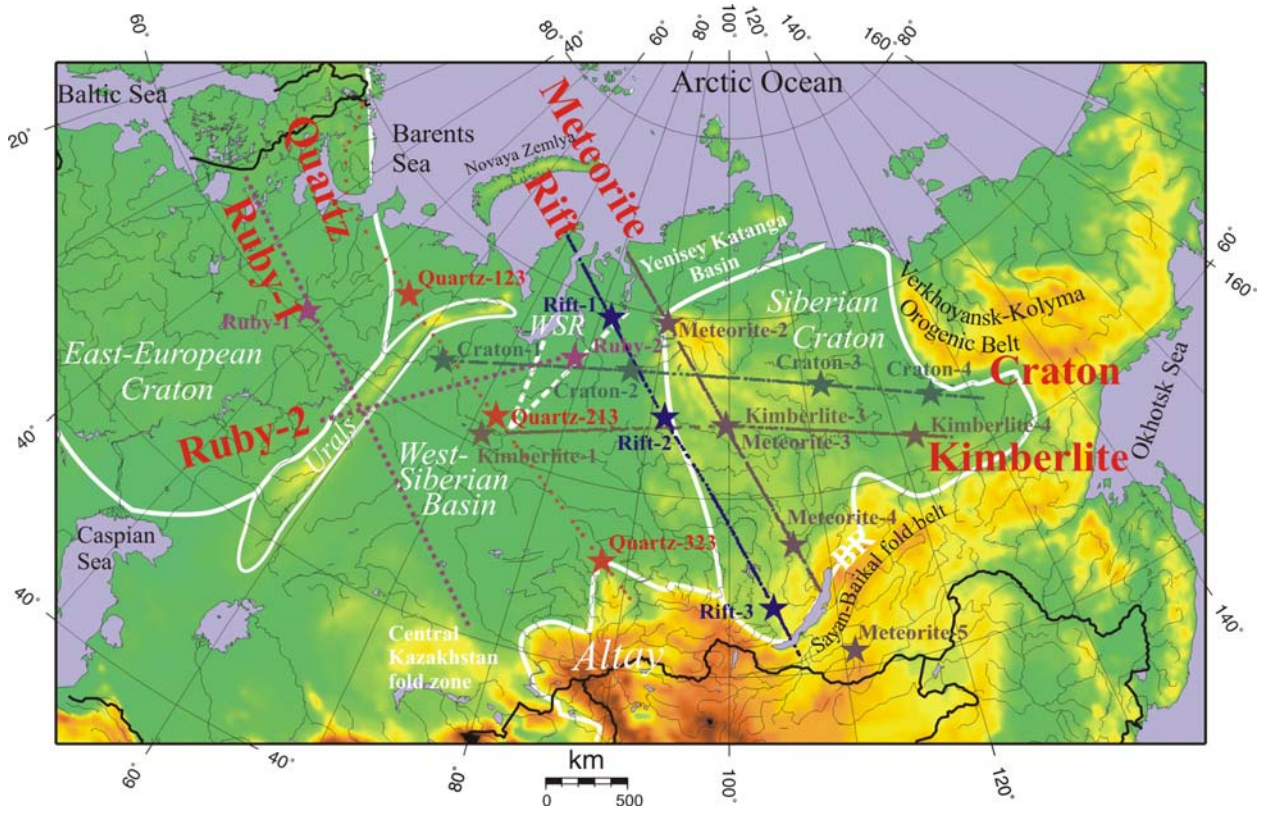

Figure 1. Six DSS projects that recorded 19 PNEs of this study. Large stars indicate the PNEs, and white shows the major tectonic boundaries (WSR – West Siberian Rift; BR – Baikal Rift) (Zonenshain, 1990). Color represents the surface elevation.

However, Northern Eurasia is also arguably the world's best-covered region with crustal and mantle-scale controlled-source seismic profiles. From the 1960s to the 1980s, the Soviet Union acquired a network of dense,

linear, long range, three-component Deep Seismic Sounding (DSS) profiles using conventional and Peaceful Nuclear Explosions (PNEs) over almost all of Northern Eurasia. In ongoing cooperation with Russian scientists, several research groups (Karlsruhe, Copenhagen, and Wyoming) have contributed to the preservation and analysis of the unique PNE datasets. At the University of Wyoming, our particular emphasis is on application of the PNE waveform recordings to nuclear test monitoring. We have obtained from Russia seven ultra-long-range profiles including 19 PNEs (Figure 1), which contribute greatly to the ground truth of the region and to the development of techniques of seismic nuclear test monitoring.

Because site effects cause strong variability of the absolute recorded amplitudes, particularly with the portable deployments of the DSS program, relative amplitudes are preferable for correlation with crustal structures. From previous studies, the *Lg* amplitude ratios, such as *Lg*/*Sn* (Sandvol et al., 2001), *Pg*/*Lg* (Philips et al., 2001), or *Lg*/*Pgcoda* (McNamara and Walter, 2001) were found to be effective in correlating with variations of crustal structure. In addition, recent studies have concentrated on studying the spectral characteristics of all the regional phases, and calibrating the sensitivity of different ratios to the variations of the crustal structure. In this work, we utilize our PNE waveform database to determine the main factors affecting *Lg* phase propagation and correlate the variations of the crustal structure in Northern Eurasia with the more sensitive amplitude ratios (*Lg*/*Sn* and *Lg*/*Pgcoda*) within the optimal frequency band.

An important advantage of PNE DSS interpretation over the traditionally used single-station recording is the ability to correlate the seismic phases over short distances of 10-20 km and within continuous offset gathers of up to 0-3800 km. In particular, in the analysis of the amplitude and spectral characteristics below, this dense recording allows us to identify and chose *P*, *S*, and *Lg* event time windows straddling the particular phases rather then rely on the

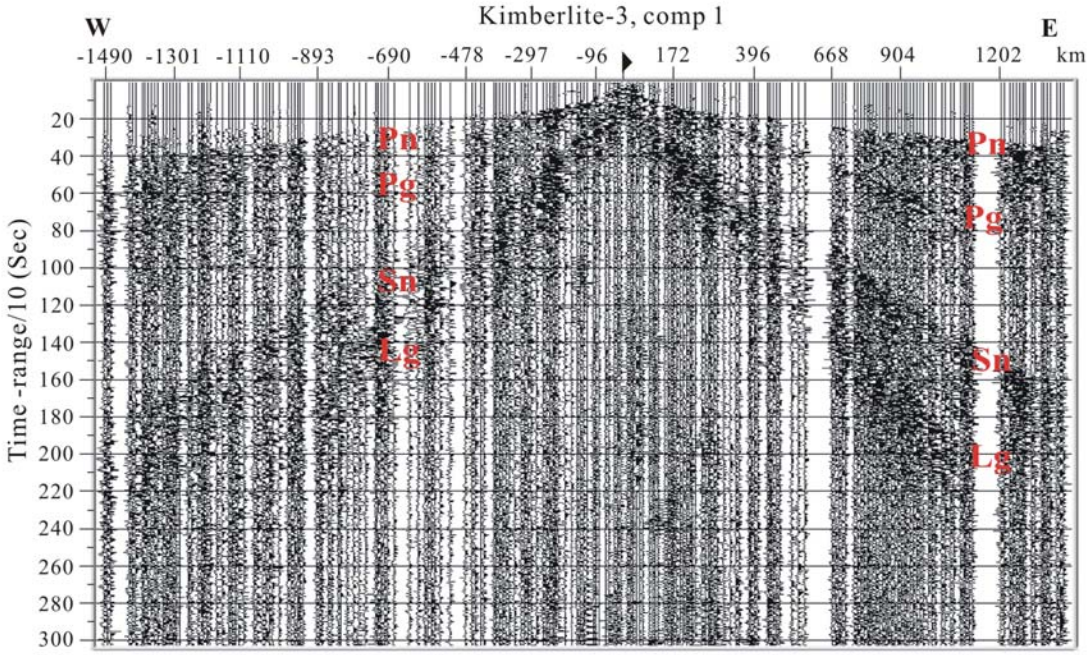

Figure 2. Inline-component seismic records from PNE Kimberlite-3 within 0.5-10-Hz frequency band. All the regional phases (*Pn, Sn, Lg, Pg*) are clear and propagate to 1000-1500-km offsets. Note the asymmetry of the phase amplitude pattern in two directions from the shot.

average group velocities as is commonly done in *Lg* studies. In the following, the event time gates are based on such carefully picked arrival onset times extended by 10-20 sec, as required by the analysis.

Spectral characteristics of regional phases

In the radial-component seismic records of Kimberlite-3 all the regional phases, *Pn*, *Pg*, *Sn* and *Lg* are clear within the recording offset range (Figure 2). To compare the *Lg* and *Sn* spectra at different offsets, we averaged the Fourier spectra of traces within 50 km around the 500- and 1000-km offsets from several PNEs (Figure 3). The *Lg* phase is mainly strong at low frequencies (<3Hz), and the *Sn* phase is strong at higher frequencies (>3Hz). Therefore, the *Lg*/*Sn* amplitude ratio is highest within the frequency band of 0.5-3 Hz, and this frequency band is used in our study.

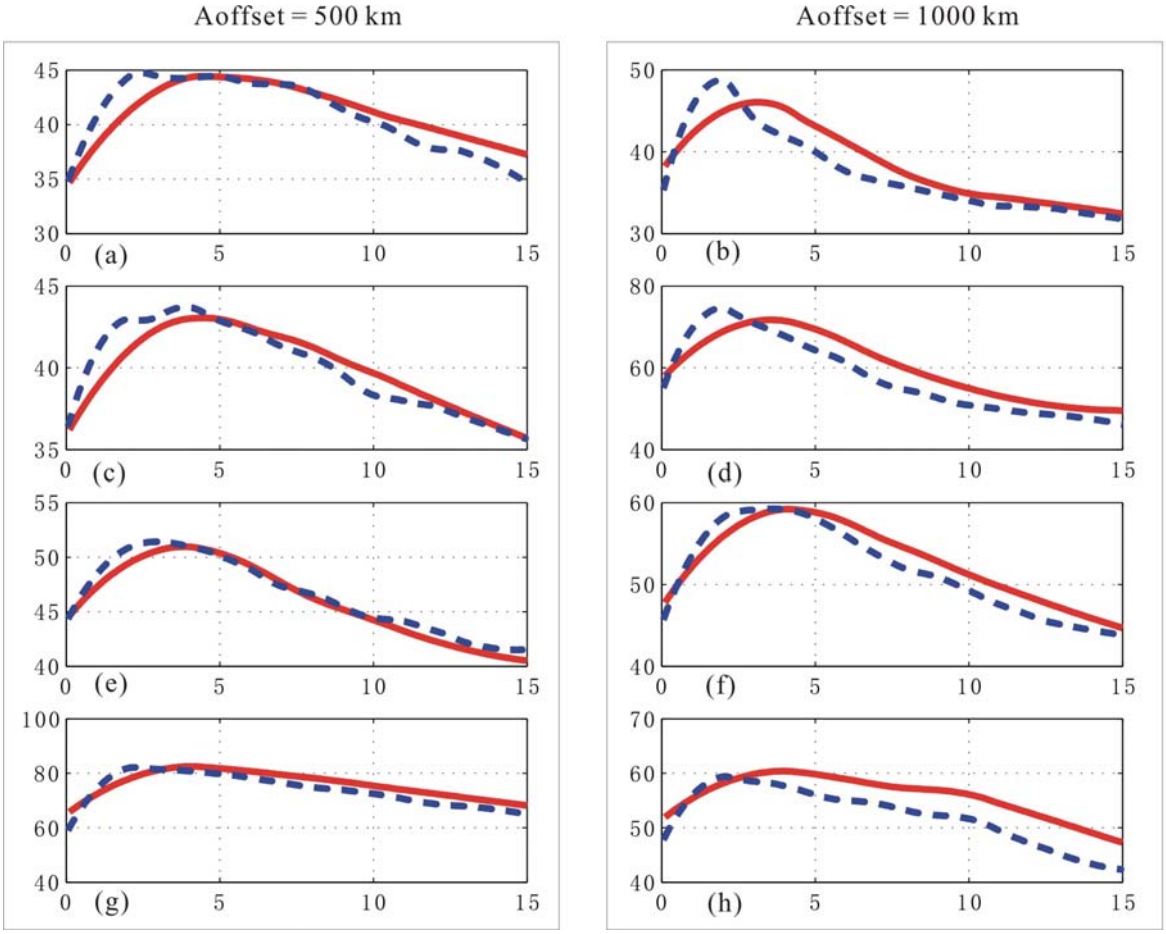

Figure 3. *Sn* (solid line) and *Lg* (dashed line) spectra at 500- and 1000-km offsets from several PNEs: a-b) Craton-3; c-d) Kimberlite-3; e-f) Meteorite-3; g-h) Kimberlite-4. Note that the peak *Lg* energy is concentrated below 3 Hz whereas the *Sn* peaks between about 3-5 Hz. Consequently, in our analysis of spatial variability of the amplitude ratios, we use the 0.5-3 Hz band in which the *Lg*/*Sn* ratios are higher.

Stability of amplitude ratios and comparison of different amplitude ratios

After picking the onset times of all the regional phases, arrival amplitudes were computed within the phase time windows. In this study, we chose the *Lg* window length to be 20 s and the *Sn* window length as 10 s. For the coda of *Pg*, we used the 10-sec window immediately before the picked onset of the *Sn* phase. For each phase, we computed amplitudes of each of the three components and combined them into a RMS vector measure, i.e., Amp = $(amp1^2 + amp2^2 + amp3^2)^{1/2}$.

Since *Lg* and *Pg* are guided waves trapped in the crust, they form only after ~300 km offset in Northern Eurasia. Therefore, the regional phases become separated after the offset of ~300 km (Figure 2), and we used only these

offsets in our analysis. By comparing the amplitude ratios obtained using different mathematical methods (RMS, median, peak, and bootstrapping) (Figure 4), we found that the resulting amplitude ratios are quite consistent, and the error from the bootstrapping method is small. The amplitude measurements and the ratios are stable and depend only on shot size, shot conditions, and travel path. By comparing the amplitude ratios (*Lg*/*Sn*, *Lg*/*Pgcoda*, *Lg*/*Pg*) (Figure 4) with the variations of the crustal structure, we found the *Lg*/*Sn* and *Lg*/*Pgcoda* were better for correlating with variations of the crustal structure and thus constraining the main factors affecting *Lg* propagation.

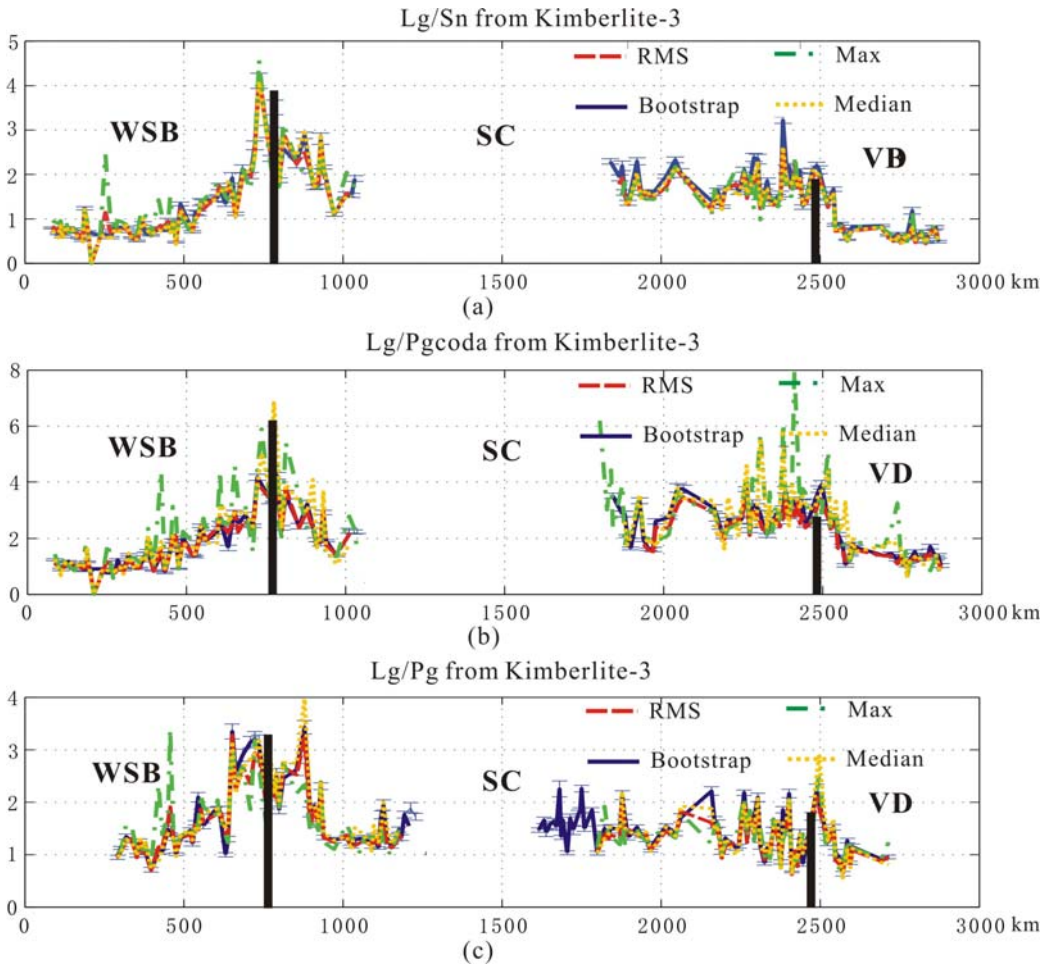

Figure 4. Comparison of several amplitude measures applied to several amplitude ratios: a) *Lg*/*Sn*, b) *Lg*/*Pgcoda*, and c) *Lg*/*Pg*. All measures produce similar results, with the exception of a somewhat less stable peak amplitude estimator (labeled as Max). Among the three amplitude ratios, the *Lg*/*Pg* is different from the other two and is less consistent with the variations of the crustal structure. Black bars are the major tectonic boundaries; WSB denotes the West Siberian Basin, SC- Siberian Craton, VD – Viluy Depression (Figure 1).

Comparison of the variations of amplitude ratios with crustal structure along profile CRATON

The Craton profile starts from the Preural High in the west, crosses the Ob-Tasovsk Depression, Yenisey Ridge, Tungass Basin, Mirninsk-Aihalsk High, and Vilui Depression, and ends in the Aldan Shield in the East (Figure 1). The complicated crustal structure provides an excellent chance to study the main factors to affect the *Lg* propagation and calibrate the amplitude ratios with the variations of crustal structure.

The *Lg*/*Sn* and *Lg*/*Pgcoda* along the Craton profile from the different PNEs (Craton-1, 2, 3, and 4) have very different amplitudes, which could be due to the source size and shot conditions (Sultanov et al., 1999). The source

spectra are different from shot to shot and different phases peak within different frequency bands. However, the spatial variations of the amplitude ratios are consistent between the different shots. We distinguish two constituents in these spatial variations: 1) regional offset dependence, and 2) local variations due to the local crustal structure. These components can potentially be separated where multiple coverage by reversed PNEs is available.

Along the profile, the amplitude ratios show systematic variations that are likely correlated with the local crustal structure. In general, it appears that the crustal thickness could be the primary factor affecting the *Lg* amplitude ratios (Figure 5). At profile distances < 900 km, both ratios decrease with offset at a rate of ~0.002/km; between ~1200 and 1500 km, the rate of their decrease becomes lower, < 0.001 /km, which could be due to a slow variation of crustal thickness. Between ~1500 to 2000 km both ratios increase with offset, in contradiction to what would be expected from the effect of the increased sediment thickness (up to 8 km, Figure 5a). This could be due to the high-velocity (4.5-5.5 km/s) and presumably low-attenuation sediments in the Tunguss Basin. Between kilometers ~2000 to ~2500 of the profile, the amplitude ratios stay constant or increase with offset, which could correspond to a thin sediment cover of the craton. At the eastern end of the profile (> 2500 km in Figure 5), the *Lg*/*Sn* and *Lg*/*Pgcoda* decrease rate is ~0.005/km, corresponding to the thick (up to 13 km), young (2.5-4.5 km/s *P*-wave velocities) sediments and pronounced Moho uplift (more than 10 km).

Note that between the profile positions of ~1000 and 1200 km, the amplitude ratios from the reversed Craton-1, Craton-3, Craton-4 PNEs are quite different. This difference can be explained if the effects of crustal thickening on *Lg* propagation are different from those of crustal thinning. A similar observation can be made between offsets ~2500 and ~2700 km (Figure 5). These preliminary observations would need to be tested and supported by further inversion and modeling.

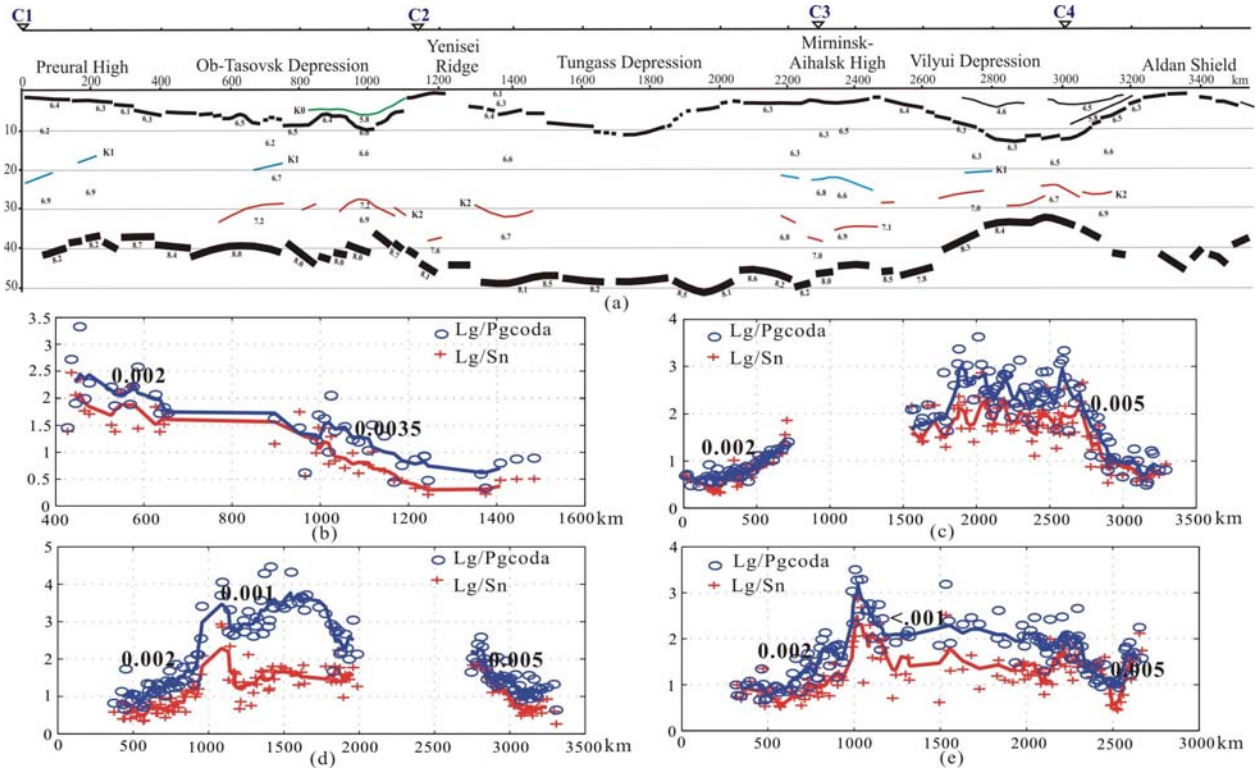

Figure 5. a) Crustal cross-section from profile Craton (Egorkin et al., 1987; Figure 1) and b-e) *Lg*/*Sn* and *Lg*/*Pgcoda* ratios from its four PNEs: Craton-1 (b), Craton-2 (c) , Craton-3 (d) , and Craton-4 (e). In cross-section a), thick black lines indicate the mapped reflecting Moho segments, red and blue lines – crustal reflections. The top of the basement is shown in black, and some reflections within the sedimentary cover are also indicated. In all plots, horizontal scales correspond to profile distance. Note the consistent variations of the amplitude ratios along the profile.

In the eastern part of the Ob'-Tasovsk Depression, a remarkable increase in the relative *Lg* amplitudes is located between kilometers 1000-1100 of the Craton profile (Figure 5). This feature still remains enigmatic; however, it could potentially be related to the complex crustal structure identified in this area, with a localized basin and a suggestion of deep crustal faulting extending to the Moho (Figure 5a). With a less consolidated crust, its response at lower (below 3-Hz) frequencies could be increased, resulting in increased relative *Lg* amplitudes. After the *Lg* waves pass this region, their amplitudes resume the "regional" trend (Figure 5d).

Variations of amplitude ratios in Northern Eurasia from seven PNE profiles

By computing the *Lg*/*Sn* and *Lg*/*Pgcoda* amplitude ratios for the 19 PNEs and correlating the ratios from the different reversed shots along the same profile, the variations of amplitude ratios in Northern Eurasia were determined along the seven profiles and summarized in Figure 6.

In the East-European Craton, along the Ruby-1 profile and Quartz profile in the Baltic Shield, the thickness of the sediments is <2 km, and the crustal thickness is ~40 km; both *Lg*/*Sn* and *Lg*/*Pgcoda* along the Ruby-1 (Ruby-1) and

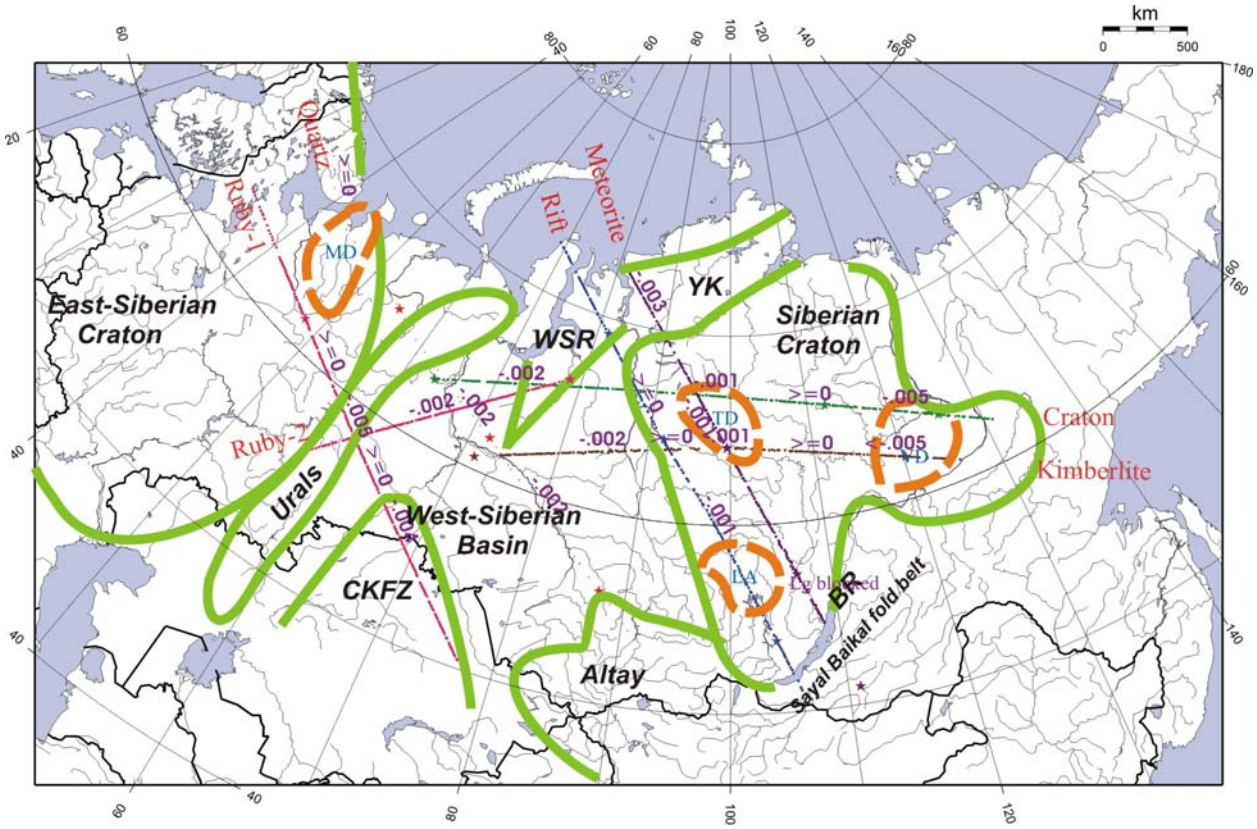

Figure 6. Sketch of tectonic boundaries (green lines) of Northern Eurasia and distribution of the observed *Lg* coda Q and *Lg* amplitude ratio-offset slopes (purple numbers). Orange contours show the areas where *Lg* appears to be blocked or highly attenuated. Labels indicate the key crustal structural features: WSR – West Siberian Rift; BR – Baikal Rift; CKFZ – Central Kazakhstan Folded Zone; YK – Yenisey-Khatanga Basin (up to 10 km of sediments); TD – Tunguss Depression (8-km sediments); LA – Low-Angara Depression (10 km of sedimentary rocks); VD – Viluy Depression (6-13 km of sediments); MD – Mezen Depression (2-5 km of sedimentary cover).

Quartz (Quartz-2, also often referred to as Quartz-123) profiles increase or are constant with offset. Under the Mezen' Depression between the Baltic Shield and the Timan Belt, the Moho is uplifted about 5 km and the sediments are ~2-5 km thick (Morozova et al., 1999); the observed *Lg/Sn* and *Lg/Pgcoda* along Quartz profile decrease with offset and the slope is ~0.002 km/s.

Three deep depressions (Viluy, Tungass, and Low-Angara) are present in the Siberian Craton. The Tungass Basin is filled with thick sediments (up to 8 km) composed of metamorphosed Paleozoic rocks mixed with plateau-basalts, and their velocities are high (~4.5-5.5 km/s) (Egorkin et al., 1987; Pavlenkova, 1996). Although the sedimentary rocks are thick in the Tungass Basin, no strong Moho uplift is observed and the crustal thickness is up to ~48 km. From Craton (Craton-2, Craton-3, Craton-4), Kimberlite (Kimberlite-3, Kimberlite-4), and Meteorite (Meteorite-4) profiles, both amplitude ratios decrease very slowly (<0.001km/s), which could correspond to the high sediment velocity and slow variations of crustal thickness. The sedimentary rocks and crust in the Low-Angara Basin have lower velocities than those in Tungass Bain, and the sedimentary rocks are up to 10 km thick. Moreover, the Moho is uplifted under this basin by ~3 km (Pavlenkova, 1996; Pavlemkova et al., 2002). From Rift PNEs (Rift-1, Rift-2, and Rift-3), both ratios in Low-Angara Basin decrease with offset and the slope is higher (~0.0015/km). The slopes of the amplitude ratios are ~0.005/km (Craton-2, Craton-3, and Kimberlite-3) in Viluy Depression, corresponding to abrupt crustal thinning (>10 km) and thick (up to 13 km), low-velocity (2.5-4.5 km/s), sediments.

Although the heat flow is high (~120mW/m^2) in the Baikal Rift Zone, no clear amplitude ratio variations are observed along the Meteorite profile (PNEs Meteorite-3 and Meteorite-5). However, for Meteorite-4 and Meteorite-5, which are near the Baikal Rift Zone, both *Lg* and especially *Sn* amplitudes are low while the *Pg* is strong; this could be due to the crustal heterogeneity that could be associated with the high heat flow region. From Craton (Craton-2, Craton-3, and Craton-4), Kimberlite (Kimberlite-3 and Kimberlite-4), and Meteorite (Meteorite-3 and Meteorite-4), along paths with thin sediments in the Siberian Craton, both ratios increase or are constant with offset.

The West-Siberian Basin is filled with young (post-Cretaceous), low-velocity (2.5-5 km/s) sediments, and the sediments are ~2-5 km thick. Steep subsidence of the basement is found in the northern part in the West-Siberian Rift (or Ob-Tanskov Depression) (up to 10 km), Yenisey-Khatanga Depression, and particularly in the Pur-Geden Basin (~13 km). The negative ratio-offset slope in the West-Siberian Basin is ~0.002/km, and ~0.003/km in the Yenisey-Khatanga Basin with its thick sediments (>10 km) and crustal thinning (~ 5 km).

The ratios decrease quickly at the Ural Mountains (~0.005/km) due to rapid crustal thickening (>10 km) and at the Central Kazakhstan folded zone (~0.004/km) with more than 5 km crustal thickening. Both ratios also decrease (~ 0.002/km) at the Mezen Depression between the Russian Plate and the Baltic Shield, which could be due to crustal thickening (< 5 km) and attenuation by the sediments.

More importantly, for the travel paths from the East-European Craton to the West-Siberian Basin across the Ural Mountains (Ruby-1 profile), and from the Siberian Craton to the West-Siberian Basin (Craton and Kimberlite profiles), both ratios increase with offset rapidly at the tectonic boundaries, and then drop quickly, perhaps because the *Lg* phase is partially blocked due to abrupt variations of crustal thickness at the tectonic boundaries.

CONCLUSIONS

The *Lg*/*Sn* and *Lg*/*Pgcoda* amplitude ratios are useful for calibration of the characteristics of *Lg* propagation with variations of crustal structure and to constrain the main factors affecting *Lg* propagation. In the DSS Peaceful Nuclear Explosion datasets in Northern Eurasia, both ratios increase or are constant with offset within the Siberian Craton and the East-European Craton, covered with thin sediments, and decrease with offset within regions with thick sedimentary covers (the Tungass Basin and Low-Angara Basin of the Siberian Craton, West-Siberian Basin, and Yenisey-Hantanga Basin). The slope of the amplitude ratios' decrease (< 0.001/km in the Tungass Basin, ~0.0015/km in the Low-Angara Basin, ~0.002/km in the West-Siberian Basin, and ~0.003km/s in the Yenisey-Hantanga Basin) could depend on both the thickness and the age of the sediments. Both ratios drop quickly where *Lg* is totally (Patom-Viluy Basin) or partially (Ural Mountains, Mezen Depression, and Central Kazakhstan folded zone) blocked, apparently by rapid variations of the crustal thickness. The *Lg* phase is mainly concentrated at low frequencies (<3 Hz), and therefore this frequency band is promising in *Lg*-based nuclear-test calibration.

REFERENCES

Baumgardt, D. R. 2001. Sedimentary basins and the blockage of Lg wave propagation in the continents. Pure and Applied Geophysics, Vol. 158, 1207-1250.

Belousov, V.V., Pavlenkova, N.I., and Kvyatkovskaya, G.N., 1992. Structure of the crust and upper mantle of the [Former] USSR. Part I, Integrated geophysical models of the major geostructures of the USSR. Vol. 34, 213-343.

Belousov, V.V., Pavlenkova, N.I., and Kvyatkovskaya, G.N., 1992. Structure of the crust and upper mantle of the [Former] USSR. Part II, Generalized geophysical data on the structure of the tectonosphere of the USSR. International Geology Review, Vol. 34, 345-444.

Egorkin, A.V., Zuganov, S.K., Pavlenkova, N.A., and Chernyshev, N.M., 1987. Results of lithospheric studies from long-range profiles in Siberia. Tectonophysics, Vol. 140, 29-47.

Kim, W.Y., et al., 1997. Discrimination of earthquakes and explosions in Southern Russia using regional high-frequency three-component data from IRIS/JSP. Bulletin of the Seismological Society of America, Vol. 87, 569-588.

McNamara, D. E., and Walter, W.R. 2001. Mapping crustal heterogeneity using Lg propagation efficiency throughout the Middle East, Mediterranean, Southern Europe. Pure and Applied Geophysics 158, 1165-1188.

Morozova, E. A., I. B. Morozov, S. B. Smithson, and L. N. Solodilov, 1999. Heterogeneity of the uppermost mantle beneath the ultra-long range profile “Quartz,” Russian Eurasia, J. Geophys. Res., 104 (B9), 20,329-20,348.

Pavlenkova, N. I., 1996. Crust and upper mantle structure in Northern Eurasia from seismic data. Advances in Geophysics, Vol. 37, 1-133.

Pavlenkova, G.A., Priestley, K., and Cipar, J., 2002. 2D model of the crust and uppermost mantle along rift profile, Siberian Craton. Tectonophysics, Vol. 355, 171-186.

Philips, W. S., et al. 2001. Application of regional phase amplitude tomography to seismic verification. Pure and Applied Geophysics, Vol. 158, 1189-1206.

Papine, R.R., and Ni, J.F., 2003. Propagation characteristics of Sn and Lg in Northern China and Mongolia. Bulletin of the Seismological Society of America. Vol. 93, 939-945.

Saikia, C. K., Woods, B.B., and Thio, H.K. 2001. Calibration of the regional crustal waveguide and the retrieval of source parameters using waveform modeling. Pure and Applied Geophysics, Vol. 158, 1301-1338.

Sandvol, E., et al. 2001. Tomographic imaging of Lg and Sn propagation in the Middle East. Pure and Applied Geophysics, Vol. 158, 1121-1163.

Sultanov, D. D., J. R. Murphy, and Kh. D. Rubinstein (1999). A seismic source summary for Soviet Peaceful Nuclear Explosions, Bull. Seism. Soc. Am., 89, 640-647.

Walter, W.R., Mayeda, K.M., and Patton, H.J., 1995. Phase and spectral discrimination between NTS earthquakes and explosions. Part I: empirical observations. Bulletin of the Seismological Society of America, Vol. 85, no.4, 1050-1067.

Volkov V.M., et al. 1984. Geology of the USSR. Publishing Office "Nauka", Moscow, 1984.

Zonenshain L.P., Kuzmin, M.I., and Natapov. B.M., 1990. Geology of the USSR: a plate tectonic synthesis. American Geophysical Union, Washington, D.C.